[Müjdat Çetin, Ivana Stojanović, N. Özben Önhon, Kush R. Varshney,

Sadegh Samadi, W. Clem Karl, and Alan S. Willsky]

Sparsity-Driven Synthetic Aperture Radar Imaging

[Reconstruction, autofocusing, moving targets,

and compressed sensing]

This article presents a survey of recent research on sparsity-driven synthetic aperture radar (SAR) imaging. In particular, it reviews 1) the analysis and synthesis-based sparse signal representation formulations for SAR image formation together with the associated imaging results, 2) sparsity-based methods for wide-angle SAR imaging and anisotropy characterization, 3) sparsity-based methods for joint imaging and autofocusing from data with phase errors, 4) techniques for exploiting sparsity for SAR imaging of scenes containing moving objects, and 5) recent work on compressed sensing (CS)-based analysis and design of SAR sensing missions.
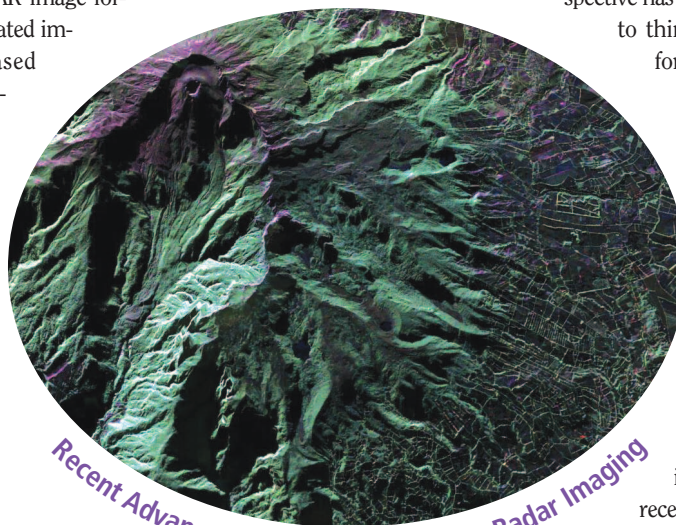

Recent Advances in Synthetic Aperture Radar Imaging

PHOTO COURTESY OF NASA

methods offering a number of benefits for SAR, including increased resolvability of point scatterers, reduced speckle, easier-to-segment regions, and robustness to limitations in data quality and quantity. Furthermore, the sparse signal representation perspective has provided inspiration for new ways to think about and produce solutions for several important problems for SAR, which are also motivated by a number of emerging SAR data collection scenarios. These problems include autofocusing, wide-angle imaging, interferometry, SAR tomography (Tomo-SAR), through-the-wall radar imaging, multiple-input, multiple-output (MIMO) radar imaging, passive radar imaging, and moving target imaging, among others. Finally, recent results on CS, built upon sparse signal representation, have generated considerable interest in radar waveform design as well as analysis and design of radar sensing scenarios under data collection constraints. Pursuing this overall new line of inquiry on SAR imaging leads to the discovery of a variety of technical problems that fall outside the standard domain of sparse signal representation, but that involve issues of critical concern for SAR imaging. The result is a rich, new area of research that has already shown its promise but that also motivates interesting lines of inquiry for the future. In this article, we present an overview of the recent line of research pursued by several research groups on sparsity-driven SAR imaging. Our article shares some aspects of two recent survey papers [1], [2]. The first of these papers [1] provides a broad introduction to the use of CS in radar,

INTRODUCTION

SAR imaging and sparse signal representation are well-established distinct lines of research. That said, sparsity has been of interest for SAR imaging implicitly over many years, and more explicitly within the last 15 years or so. In fact, a considerable fraction of recent developments for SAR imagery have been driven by moving from a purely Fourier transform type processing paradigm to one that couples physics-motivated sensing models with some form of sparsity-based priors. Ideas based on sparse signal representation, proposed by a number of research groups, have recently led to advanced image formation

and considers three applications: pulse compression, radar imaging, and air space surveillance with antenna arrays. The second paper [2] provides an overview and examples of how central themes in sparsity and CS have been present in the array processing literature in general, and in radar imaging in particular, over many years. Our article complements these papers in several ways and presents a focused and up-to-date picture of sparsity-driven radar imaging. In particular, we provide a comprehensive coverage of recent use of sparsity in a variety of radar imaging scenarios, with a signal processing focus and perspective. Applications and connections covered include wide-angle imaging, autofocusing, moving target imaging, as well as CS.

ANALYSIS AND SYNTHESIS-BASED SPARSE RECONSTRUCTION FOR SAR

SAR imaging can be viewed as a linear inverse problem in which an unknown spatial reflectivity field is reconstructed from noisy measurements of waves backscattered from a scene. After certain steps of preprocessing of the radar returns, the resulting data can be related to the underlying reflectivity field through a discretized model of the following form, which essentially involves a spatial Fourier transform:

$$r(f_k, \theta_l) = \sum_{m=1}^{M} s(x_m, y_m) e^{-j\frac{4\pi f_k}{c}(x_m \cos\theta_l + y_m \sin\theta_l)} + n(f_k, \theta_l), \quad (1)$$

where c denotes the speed of light. We can stack the entire set of noisy phase history measurements $r(f_k, \theta_l)$, and the noise $n(f_k, \theta_l)$ at all available frequencies f_k, $k = 1, \ldots, K$, and viewing angles θ_l, $l = 1, \ldots, L$, as well as the reflectivity function or scattering response $s(x_m, y_m)$ at all spatial locations (x_m, y_m), $m = 1, \ldots, M$ (which include all the points containing the non-negligible scatterers), into vectors to obtain the following observation model:

$$\mathbf{r} = \mathbf{Hs} + \mathbf{n}, \quad (2)$$

where $\mathbf{s}$ denotes the underlying, complex-valued reflectivity image and $\mathbf{H}$ is the mathematical model of the observation process described by (1). While this model and the ideas described in this article can be used in the context of a variety of SAR operating modes, for basic SAR imaging we will mostly assume spotlight-mode operation for concreteness. Given limitations in the bandwidth of the measured data and in the diversity of look angles, as well as the inherently noisy nature of the measurement process, the inverse problem in (2) is ill posed. To generate a solution, implicit or explicit assumptions need to be made. Principled ways to incorporate such assumptions, in the form of constraints or prior information, include regularization and Bayesian estimation methods. Within this context, the information or constraint that the underlying reflectivity field admits a sparse representation has proved to be a very useful asset for SAR imaging. The simplest form of sparsity (or compressibility) to exploit would be a scene consisting of a small number of dominant scatterers (e.g.,

man-made metallic objects). Exploitation of this type of sparsity has led to superresolution imaging in SAR (see Figure 1) [56]. More generally, the scene could be sparse in a different domain, as we discuss in more detail below. The remainder of this section provides an overview of analysis and synthesis-based sparse signal representation methods applied to SAR imaging.

In an analysis model, sparsity is imposed on some transformation or features of the signal of interest, and, in this case, is often called *cosparsity*. Such an approach for SAR imaging was proposed in [3], where an estimate of $\mathbf{s}$ is obtained by minimizing the following cost functional:

$$J(\mathbf{s}) = \|\mathbf{r} - \mathbf{Hs}\|_2^2 + \lambda_1 \|\mathbf{s}\|_p^p + \lambda_2 \|\nabla|\mathbf{s}|\|_p^p. \quad (3)$$

Here $\|\cdot\|_p$ denotes the ℓ_p-norm, ∇ is a discrete approximation to the two-dimensional (2-D) derivative operator (gradient), $|\mathbf{s}|$ denotes the vector of magnitudes of the complex-valued vector $\mathbf{s}$, and λ_1 and λ_2 are scalar parameters. For $p < 2$ we have promotion of sparsity, which gets weaker as we approach $p = 2$. The values used for p in sparsity-driven SAR imaging are around 1, so the second and third terms enforce sparsity. The relative contribution of these two terms are determined through the choice of the hyperparameters λ_1 and λ_2. The second term indicates a preference for spatially sparse reflectivity fields. The third term enforces sparsity on the gradient of the reflectivity magnitudes, indicating a preference for piecewise smooth reflectivity magnitude fields. Such piecewise smoothness constraints have a long history in real-valued image restoration and reconstruction, under various names including edge-preserving regularization and total variation restoration. Within the context of SAR imaging, such smoothness is expected within homogeneous natural terrain types and within some man-made structures. Even in homogeneous regions, the phases of the reflectivities in spatially neighboring pixels however are generally uncorrelated, hence no such smoothness is expected in phase. As a consequence, we need to impose sparsity on $\nabla|\mathbf{s}|$, and not on $\nabla\mathbf{s}$, as the latter would lead to smoothing of the real and imaginary parts of the reflectivity field, which may not lead to the desired smoothing effect on the magnitudes.

Another perspective on sparsity-driven SAR imaging is that it can be used to preserve and enhance features that might be used in decision making based on SAR images, such as automatic target recognition. With this perspective, the image formation approach of (3) was called *feature-enhanced imaging* in [3], with a dominant second term leading to *point-enhanced imaging* and a dominant third term leading to *region-enhanced imaging*. Point-enhanced imaging provides improved resolvability in sparse scenes, an example of which is provided in Figure 1. Region-enhanced imaging imposes sparsity on spatial gradients and leads to images with reduced speckle and easier to segment regions. Such improvements have partially been quantified in terms of feature extraction accuracy and object classification performance [4], [5].

Having to use a penalty on the magnitudes makes the optimization problem in (3) more challenging than its counterparts in real-valued sparse signal recovery problems. Efficient algorithms
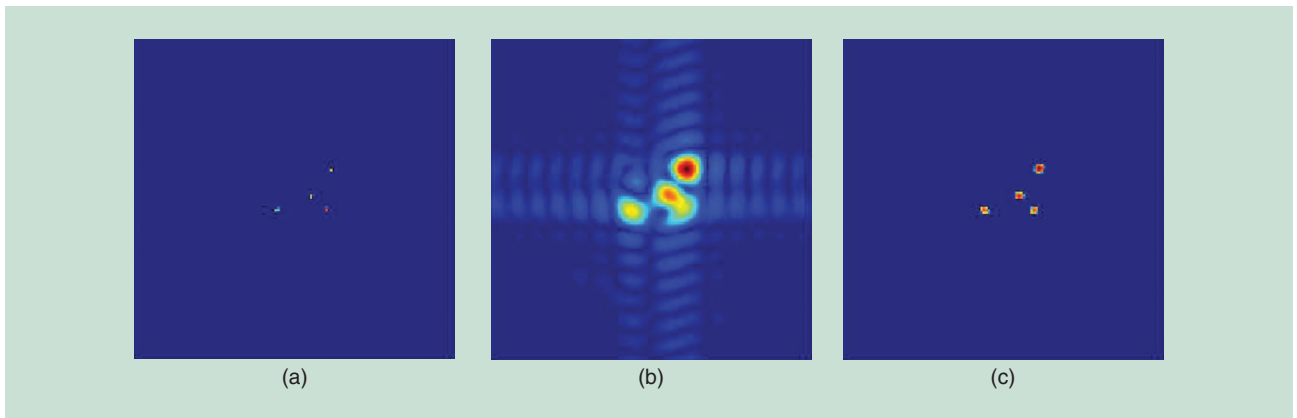
[FIG1] The reconstructions of the slicy target from the MSTAR data set [56]. (a) The reference image reconstructed from high-bandwidth data. (b) The conventional image reconstructed from limited-bandwidth data. (c) The sparsity-driven, point-enhanced image reconstructed from limited-bandwidth data.

matched to this problem structure have been developed [3]. These algorithms are based on half-quadratic regularization, and can be viewed as quasi-Newton methods with a specific Hessian update scheme. Another interpretation is that the overall nonquadratic problem is turned into a series of quadratic problems, each of which is efficiently solved in each iteration using conjugate gradients. The special case of point-enhanced imaging can be solved by a variety of algorithms developed for sparse signal representation. In [6], a fast and adaptive sequential basis selection strategy is employed for point-enhanced imaging. Rather than solving a basis pursuit type optimization problem for point-enhanced SAR imaging, an alternative is to use a greedy matching pursuit algorithm, as in [7] and [8]. While the development of computationally efficient algorithms matched to the problem structure has been and continues to be an important line of research, at the fundamental level, the cost of solving the optimization problems involved in sparsity-driven SAR imaging is significantly higher than conventional processing. Hence there is certainly a price to be paid for potential improvements obtained in image quality. We should also note that many cost functionals considered in sparsity-driven SAR imaging are nonconvex. Throughout the work surveyed in this article, local optimization algorithms aiming to find the local minima of such cost functionals are used.

Now let us turn to synthesis-based models for sparse representation. In a synthesis model, the formulation is based on representing the signal of interest in terms of a dictionary and imposing sparsity on the dictionary coefficients. Let us just focus on one appealing feature of a synthesis model in the context of SAR imaging. We note that (3) uses two different regularization terms, one imposing the spatial sparsity of the field, and the other its piecewise smoothness. (One could combine the two terms into a single terms using a "tall" operator carrying out both analysis operations.) These two terms are used together to handle cases in which one of these terms does not serve as a good enough constraint throughout the scene. However, (3) imposes these two potentially conflicting constraints jointly everywhere in the scene, leading to some degree of inconsistency with the stated objective. This issue may be handled in a more consistent manner

within a synthesis model. In particular, one can form an overcomplete dictionary consisting of atoms corresponding to the different types of features represented by the two constraints in (3). As the atoms can also exhibit spatial locality, one or the other type of feature can be "active" at a particular location in the scene, avoiding simultaneous use of potentially conflicting constraints. This could lead to a sparser representation for scenes exhibiting different types of features at different spatial locations. Based on these thoughts, a synthesis model for sparsity-driven SAR imaging has been proposed in [9]. As in (3), what admits sparse representation is the magnitude of the reflectivity field $\mathbf{s}$. Hence we are interested in a representation of the form $|\mathbf{s}| = \mathbf{D}\boldsymbol{\alpha}$, where $\mathbf{D}$ is an overcomplete dictionary with the coefficient vector $\boldsymbol{\alpha}$. Let us also write $\mathbf{s} = \boldsymbol{\Phi}|\mathbf{s}|$, where $\boldsymbol{\Phi}$ is a diagonal matrix, the ith diagonal element of which is $e^{j\gamma_i}$, with γ_i indicating the unknown phase of the ith scene element $\mathbf{s}_i$. Based on this notation, we can rewrite the observation model as

$$\mathbf{r} = \mathbf{Hs} + \mathbf{n} = \mathbf{H}\boldsymbol{\Phi}\mathbf{D}\boldsymbol{\alpha} + \mathbf{n}. \qquad (4)$$

Letting ϕ be a vector consisting of the diagonal elements of $\boldsymbol{\Phi}$, we can write the following cost functional to be minimized for SAR imaging:

$$J(\boldsymbol{\alpha}, \phi) = \|\mathbf{r} - \mathbf{H}\boldsymbol{\Phi}\mathbf{D}\boldsymbol{\alpha}\|_2^2 + \lambda\|\boldsymbol{\alpha}\|_p^p \quad s.t. \quad |\phi_i| = 1 \quad \forall i. \quad (5)$$

We note that the variables to be optimized involve the phase of the field, and the representation coefficients of its magnitude. This problem can be solved using the coordinate descent algorithm developed in [9]. Figure 2 contains a sample reconstruction using a wavelet transform-based dictionary based on TerraSAR-X data [57]. For examples of other dictionaries used in this framework, including ones that are better matched to the task of representing reflectivity magnitudes, see [9]. This approach provides the capability to preserve and enhance multiple distinct features on different spatial regions of the scene utilizing combinations of a variety of standard and custom-made signal dictionaries including contourlets, combination of spikes
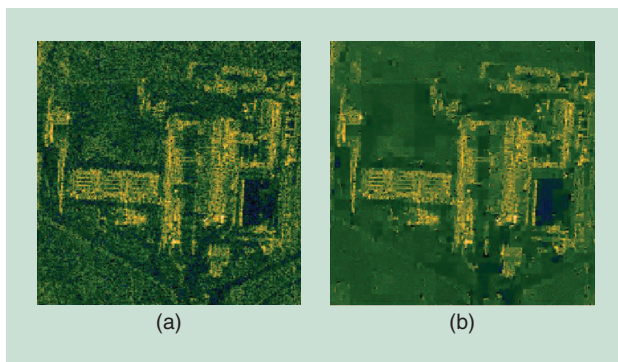
[FIG2] Reconstructions of a scene based on TerraSAR-X data [57]. (a) A conventional image. (b) A synthesis-based sparsity-driven image reconstructed using a multiresolution wavelet dictionary.

(the canonical basis to represent strong point scatterers) and edges, as well as dictionaries of various geometric shapes matched to the expected scene structure. Furthermore, the synthesis-based approach can be used to combine a standard dictionary with a learning-based dictionary. For example, [10] combines spikes with a learned dictionary. The reconstructed SAR scene would then be a composite image that can be decomposed into multiple components represented by each dictionary, as illustrated in Figure 3.

While the sparsity-driven SAR imaging problem was formulated as a regularized optimization problem above, it could alternatively be viewed as a maximum a posteriori (MAP) estimation problem with a Bayesian perspective, in which the sparsity constraint turns into a heavy-tailed prior distribution for the features of interest. Continuing with the Bayesian perspective, one could also be interested in choosing other costs, leading to other estimators than MAP, or characterizing the posterior density rather than finding just a point estimate. There has been some exploration in this direction [11], [12]. There also exists some preliminary work on automatic regularization parameter selection for sparsity-driven SAR imaging [13].

Sparsity-driven SAR imaging has been extended to and applied in emerging sensing scenarios in which the sensing aperture or the data are limited or sparse in some sense (see the section "Compressed Sensing-Based Analysis and Design of SAR Sensing Missions"), as well as in multistatic active and passive radar [14] including MIMO architectures [15]. The benefits provided by sparsity-driven imaging are even greater in such nonconventional sensing scenarios. Sparsity-driven imaging has also been used for the problem of inverse SAR (ISAR) imaging of rotating targets [16], as well as for through-the-wall radar imaging [17]. It has also been extended to interferometric SAR [18] and SAR tomography (TomoSAR) [19] adding the elevation direction into the problem for 3-D imaging, as well as to four-dimensional (4-D) (differential, i.e., space-time) TomoSAR [20]. Sparsity-driven three-dimensional (3-D) image formation has also been used to initialize the process of geometric feature extraction from SAR data collected over arbitrary, monostatic or bistatic SAR apertures [21].

## WIDE-ANGLE SAR IMAGING OF ANISOTROPIC SCATTERING

Wide-angle SAR, a SAR modality in which radar returns are collected over a large azimuth extent or long aperture, has become possible due to advances in navigation and avionics that permit aircraft to follow precise routes for long distances. In theory, the wider the aspect angle covered by the synthetic aperture is, the finer the resolution of images in the cross-range direction can be. However, there are two main issues that arise in wide-angle SAR image formation. First, the sampling pattern of the collected radar returns in the frequency domain takes on an arch shape. However, the conventional Fourier transform-based polar format algorithm [22] is predicated on the polar frequency sampling pattern being a good approximation to a rectangular sampling pattern, which is violated with wide-angle apertures. Violation of this assumption leads to an irregular point spread function and to artifacts in imagery formed by conventional processing.

The second issue, and the main point of discussion in this section, is that when objects are viewed from diverse aspect angles, they have different scattering behaviors, i.e., the scattering response is a function of the azimuth angle. Imagine an upright flat metal plate; it will reflect radar signals back to the receiver strongly when viewed straight on but weakly when viewed obliquely. Angle-dependent scattering, termed *angular anisotropy*, is only prominent with wide-angle apertures, not narrow-angle apertures, in which case it is a reasonable assumption that scattering amplitude is constant over the aperture. The failure to model anisotropy in conventional image formation algorithms results in an averaging of scattering response over angle, leading to inaccurate scattering estimates in the formed imagery. Moreover, as anisotropy of scatterers is not characterized, one misses the opportunity of using it as a feature for automatic target recognition and scene understanding.

The problems of detecting, estimating, and modeling aspect-dependent scattering behavior have recently been studied. Anisotropy characterization methods may be broadly categorized into those employing parameterizations for angle-dependent scattering in the phase history domain, multiaperture methods that operate in the image domain, and sparsity-driven nonparametric image formation and anisotropy characterization methods. Within the third category, techniques either apply sparse reconstruction methods described in the previous section independently on a set of (possibly overlapping) small subapertures [8], [23]–[25] or jointly process wide-aperture data by incorporating prior information on aspect-dependent scattering [26]–[28]. The independent processing methods have similarities with image domain multiaperture methods. In the remainder of this section, we describe one example formulation of a sparsity-driven subaperture approach and two formulations of joint processing: one analysis based and one synthesis based.

Let us consider the following discrete version of the measurement model with anisotropy:

$$r(f_k, \theta_l) = \sum_{m=1}^{M} s(x_m, y_m; \theta_l) e^{-j\frac{4\pi f_k}{c}(x_m\cos\theta_l + y_m\sin\theta_l)} + n(f_k, \theta_l), \quad (6)$$
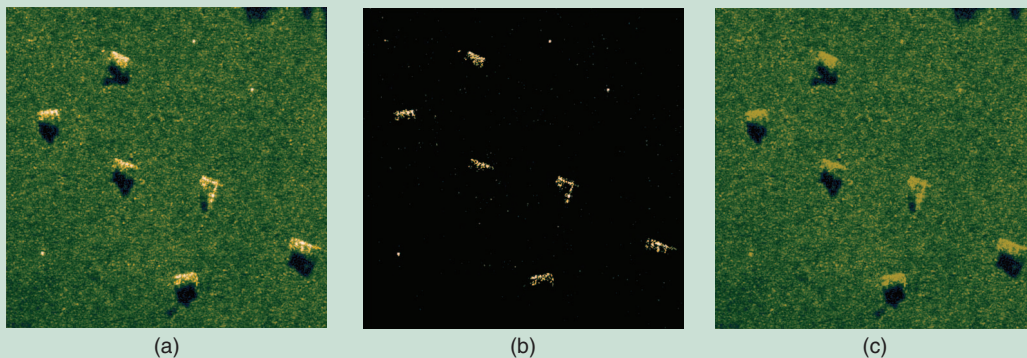
[FIG3] Reconstruction of a scene from the MSTAR data set [56] using a synthesis-based sparse representation approach combining the canonical (spike) dictionary with a learned dictionary. (a) A composite image containing six military vehicles and three corner reflectors. (b) A component consisting of strong scatterers represented by the spike dictionary. (c) A component represented by the learned dictionary. (Figure used with permission from [10].)

where $k = 1, \ldots, K$, and $l = 1, \ldots, L$. The difference from the previous section is the scattering response now being a function of the viewing angle $s(x_m, y_m; \theta_l)$. In the narrow-angle setting, the entire set of phase history measurements $r(f_k, \theta_l)$ is inverted to obtain the isotropic scattering response $s(x_m, y_m)$. For the wide-angle case, if we assume isotropic scattering within small ranges of azimuth angles, we can perform the inversion separately on intervals of θ to obtain I separate subaperture images $s_{\tilde{\theta}_i}(x_m, y_m)$ centered at angles $\tilde{\theta}_i$, $i = 1, \ldots, I$ [23]. The ranges of angle, which may overlap from one subaperture image to the next, lead to I linear systems of equations $r_{\tilde{\theta}_i} = H_{\tilde{\theta}_i} s_{\tilde{\theta}_i} + n_{\tilde{\theta}_i}$, where $r_{\tilde{\theta}_i}$ represents the subset of phase history measurements corresponding to the subaperture centered at $\tilde{\theta}_i$, $H_{\tilde{\theta}_i}$ is the corresponding subset of forward operations, and $s_{\tilde{\theta}_i}$ is the ith subaperture image we would like to find. Using methods described in earlier sections, one can reconstruct point-enhanced subaperture images by minimizing

$$J(s_{\tilde{\theta}_i}) = \| r_{\tilde{\theta}_i} - H_{\tilde{\theta}_i} s_{\tilde{\theta}_i} \|_2^2 + \lambda \| s_{\tilde{\theta}_i} \|_p^p, \quad i = 1, \ldots, I. \quad (7)$$

The resulting set of subaperture images can then be stacked and viewed as a 3-D volume in the two spatial dimensions and the angular dimension. Also, in a generalized likelihood ratio test fashion, a composite image can be formed by taking the maximum magnitude (over angles) at each pixel location [23], on which one might also use color coding to display dominant angular response directions of scatterers. Noncoherent combination of subaperture images is also studied in [24]. Motivated by a number of applications including foliage penetration (FOPEN) radar, this approach has also been shown to be effective on data with frequency-band omissions. The idea of independent processing of small subapertures described above has recently been applied in the context of 3-D circular SAR with little elevation diversity, where improved image quality is attributed to scattering center sparsity that is incorporated into the algorithms [5], [8], [25]. A sample 3-D imaging result from [25] is shown in Figure 4.

The forming of independent subaperture images fails to take prior information about the expected angular behavior of scatterers into account. In particular, point scatterers resulting from natural and man-made objects tend to have contiguous intervals of strong scattering response as a function of angle. Although each scatterer has limited persistence over the full wide-angle aperture, there exists a high correlation in magnitude response at closely spaced aspect angles within its persistence interval. Therefore, an improvement over independent reconstruction of subapertures is joint reconstruction of all subaperture images with an additional regularization term penalizing the ℓ_q-norm, $q \leq 1$, of the change in scattering magnitude at each spatial location across subaperture images [27]. The cost functional for such analysis-based joint (point-enhanced) processing is

$$J(s_{\tilde{\theta}_1}, \ldots, s_{\tilde{\theta}_l}) = \sum_{i=1}^{I} \| r_{\tilde{\theta}_i} - H_{\tilde{\theta}_i} s_{\tilde{\theta}_i} \|_2^2 + \lambda_1 \sum_{m=1}^{M} \left(\sum_{i=1}^{I} |s_{\tilde{\theta}_i}(x_m, y_m)|^2 \right)^{p/2}$$

$$+ \lambda_2 \sum_{i=1}^{I-1} \| |s_{\tilde{\theta}_{i+1}}| - |s_{\tilde{\theta}_i}| \|_q^q, \quad (8)$$

where p is chosen to be around 1 to promote sparse solutions. The second term imposes spatial sparsity on the total scattering magnitude response collected over all aspect angles, whereas the third term enforces piecewise smoothness of the scattering magnitude in the angular dimension.

An alternative synthesis-based joint processing to take the prior information on contiguity of angular persistence into account constructs an overcomplete dictionary representation for the angular dimension with atoms that are zero over some aspect angles and positive-valued over contiguous ranges of aspect angles [26]. There are no subaperture images in this approach. Specifically, for a single spatial location, the anisotropic scattering function is expanded as

$$s(x_m, y_m; \theta_l) = \sum_{n=1}^{N} a_{m,n} b_n(\theta_l), \quad (9)$$

where the $a_{m,n}$ are coefficients and the $b_n(\theta_l)$ are atoms. For each spatial location, there is one atom for each possible angular persistence width within the wide-angle aperture and each possible center angle. With such a dictionary construction, the number of atoms per spatial location is quadratic in L, the number of aspect angles in the aperture. Substituting the dictionary expansion (9) into the anisotropic phase history expression (6), and stacking all data points into vector form yields an underdetermined system of linear equations of the form $\mathbf{r} = \boldsymbol{\Psi}\mathbf{a}$, where $\mathbf{a}$ is a vector of all coefficients in the problem. The overcomplete dictionary at each spatial location can represent all contiguous angular scattering functions with a single atom. Hence in addition to spatial sparsity, the anisotropic scattering at each pixel can, in principle, be sparsely represented as well. So the problem is solved using sparsity regularization by minimizing

$$J(\mathbf{a}) = \| \mathbf{r} - \boldsymbol{\Psi}\mathbf{a} \|_2^2 + \lambda \| \mathbf{a} \|_p^p, \qquad (10)$$

where p is chosen to be around 1. Because of the quadratic number of atoms in the number of aspect angles, it is not tractable to optimize (10) directly, however the nesting structure of the dictionary allows the optimization to be approximated using a greedy graph search procedure [26]. Another challenge posed by a very large dictionary is that the problem becomes more underdetermined and it becomes harder to guarantee perfect recovery. The atomic decomposition allows for a direct interpretation of the coefficients in terms of the persistence and center angle of scattering centers. This idea can be taken a step further by setting the dictionary atoms to be canonical scattering response magnitudes from typical object geometric configurations [28].

Image formation and anisotropy characterization from wide-aperture data collection using sparsity-driven approaches leads to improved results over conventional Fourier-based methods. We illustrate this point by showing results on a 110° aperture data set corresponding to a scene containing a backhoe loader [58]. Numerical quantifications of algorithm performance may be found in the respective papers [23], [26], and [27]. In this data set, the radar signals are generated using a high fidelity electromagnetic scattering code. Backhoe results from the conventional, independent point-enhanced subaperture, joint subaperture

[FIG4] Sparsity-driven 3-D SAR imaging of a car. (a) Isometric view. (b) Side view. (c) Top view. (Figure used with permission from [25].)

reconstruction, and overcomplete dictionary algorithms are shown in Figure 5 (b)–(e), respectively. The image formed by conventional processing is quite unresolved and full of artifacts—it is difficult to even discern that the scene contains a backhoe. The backhoe is much more recognizable in the sparsity-driven results. Among the sparsity-driven approaches, joint processing gives finer resolution of the scattering behavior. The approaches we have described produce more than 2-D reflectivity images, in particular, these methods essentially reconstruct an angular scattering response at each pixel, leading to anisotropy characterization. This is demonstrated in Figure 6 for the analysis-based joint processing approach of [27]. The figure shows varying persistence of scattering as a function of angle in different parts of the backhoe. Such information could not be recovered by conventional image formation methods and could serve as an important feature for automatic target recognition and scene understanding.

IMAGING AND AUTOFOCUSING IN THE PRESENCE OF PHASE ERRORS

Phase errors in SAR phase history data arise due to errors in the estimation of the time required for the transmitted signal to propagate from the SAR platform to the scene and back. The most common causes of inaccuracies on the roundtrip propagation time are SAR platform position uncertainties and propagation induced errors due to atmospheric effects. The implication of such errors on conventional SAR imagery is the convolution of the image with a blurring kernel. Because of the defocusing effect of such errors, techniques developed for removing phase errors are called autofocus techniques. Existing well-known autofocus techniques commonly postprocess conventionally reconstructed defocused images to estimate the phase errors. One of these state-of-the-art techniques is mapdrift autofocus [29] which uses subaperture data to estimate the phase errors. Subaperture based techniques are suitable mostly for quadratic and slowly varying phase errors across the aperture. One of the most widely used autofocus techniques, phase gradient autofocus (PGA) [30], estimates phase errors using the data obtained by isolating several defocused targets via center-shifting and windowing operations. Another well-known approach for autofocusing is based on the optimization of a sharpness metric. Commonly used metrics are entropy or square of the image intensity. A relatively new autofocus technique, multichannel autofocus, is based on a noniterative algorithm that finds the focused image in terms of a basis formed from the defocused image, relying on a condition on the image support to obtain a unique solution.

The SAR autofocus problem has recently been handled in the context of sparsity-driven imaging as well. In [31], phase error estimation is performed by comparing and aligning sparsity-driven images produced from a sequence of smaller coherent processing intervals, for which motion errors can be assumed to be tolerable. For sparse aperture ISAR imaging, [32] proposes first to remove the phase errors by a weighted eigenvector-based phase correction method and then to form the image by sparsity-driven imaging. The study in [33] demonstrates the effects of phase errors on sparsity-driven imaging and presents results
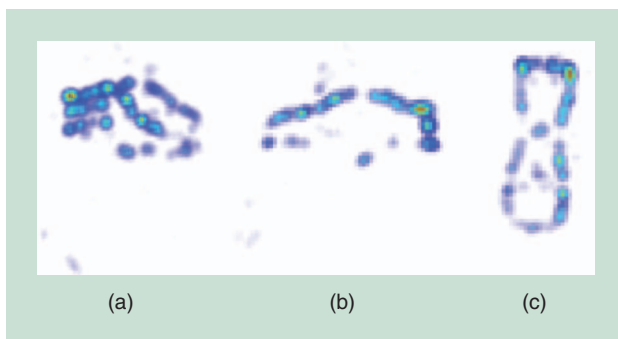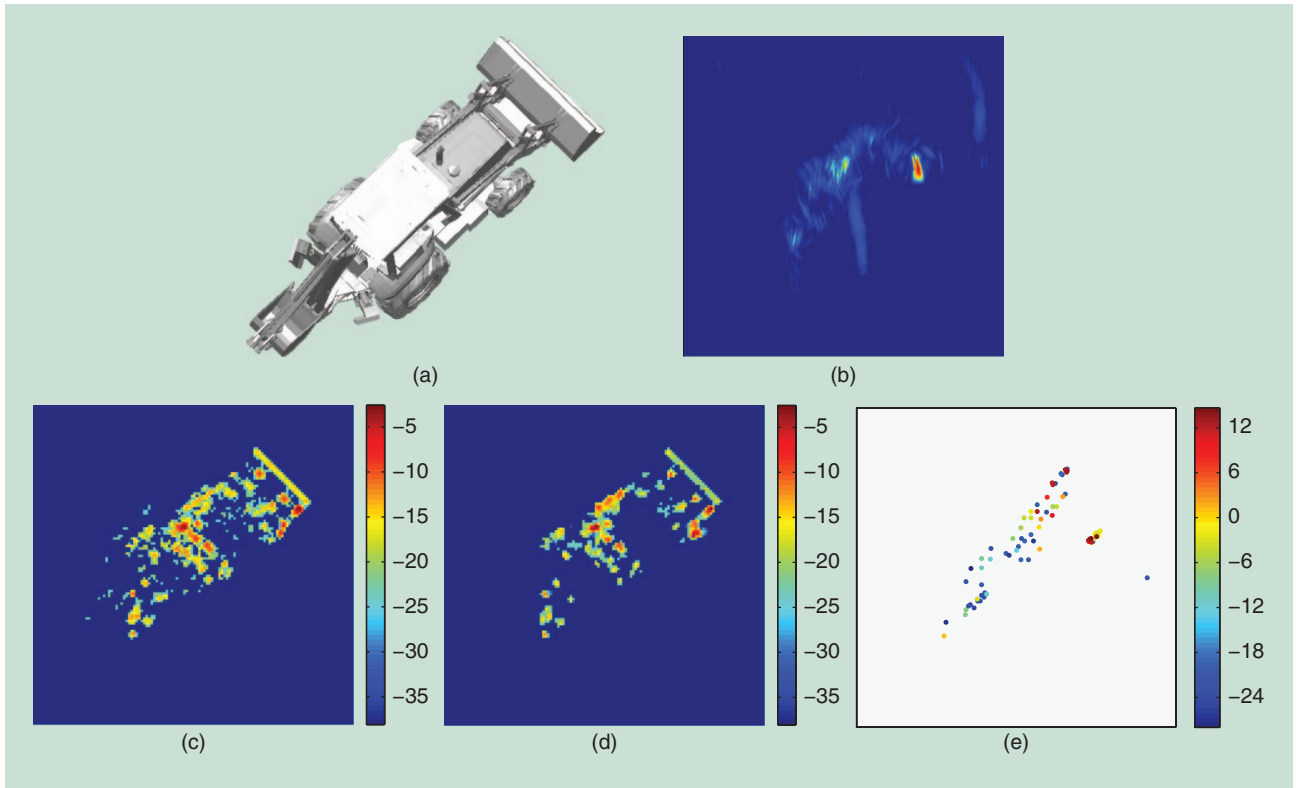
[FIG5] Wide-angle SAR imaging of a backhoe loader. (a) A CAD model. (b) Conventional reconstruction. (c) A composite independent subaperture image. (d) A composite joint subaperture image imposing piecewise smoothness in angular scattering. (e) A composite joint subaperture image based on an overcomplete dictionary for angular scattering. (Images used courtesy of [26] and [27].)

obtained by implementing PGA on sparsity-driven reconstructions. In these pieces of work, the process of sparsity-driven imaging and that of autofocusing are rather isolated.

Going one step further, one can perform autofocusing and imaging simultaneously in a sparsity-driven framework, which has been shown to produce promising results [5], [34]–[37]. As an example of such an approach, the sparsity-driven autofocus (SDA) method [34] for an isotropic scattering scenario is based on the following observation model in which phase errors are considered as model errors:

$$r = H(\epsilon)s + n. \tag{11}$$

Here, $H(\epsilon)$ denotes the model matrix that takes the phase errors ϵ into account. Assuming spatial sparsity of the reflectivity field, the following cost functional is minimized over both the field and the phase errors using a coordinate descent approach:

$$J(S, \epsilon) = \| r - H(\epsilon)s \|_2^2 + \lambda \| s \|_1. \tag{12}$$

Hence, SDA estimates the phase errors and performs sparsity-driven imaging jointly by solving this optimization problem. SDA has been used to compensate a variety of commonly encountered types of phase errors. A sample result on the backhoe data for a case involving randomly varying phase errors along the aperture

with a uniform distribution in $[-\pi, \pi]$, is displayed in Figure 7. Note that this is a wide-angle imaging scenario and SDA is applied on subapertures within the framework of the wide-angle imaging method of [23]. Figure 7(a) and (b) show the reconstructions obtained by conventional imaging, and direct application of sparsity-driven imaging without phase error compensation, respectively. The result of joint sparsity-driven imaging and phase error compensation through SDA is shown in Figure 7(c), which demonstrates the effectiveness of SDA in removing phase errors and reconstructing a high-quality image. The experimental analysis in [34] also shows how SDA provides improvements over existing autofocus methods.

More recently, [35] and [36] have used similar ideas to achieve autofocusing of undersampled SAR data. The method proposed in [35] is based on minimizing a constrained version of the cost functional in (12). Optimization is performed through a three-block relaxation approach by using an extra surrogate parameter for the field to guarantee convergence. In [36], motion compensation and image reconstruction are performed for SAR data obtained at a fraction of the Nyquist rate using reduced rate analog-to-digital converters. A total variation penalty on the field is incorporated into the optimization problem as well. In [37], the idea of joint sparsity-driven imaging and autofocusing is used for 3-D imaging based on undersampled linear array SAR data.
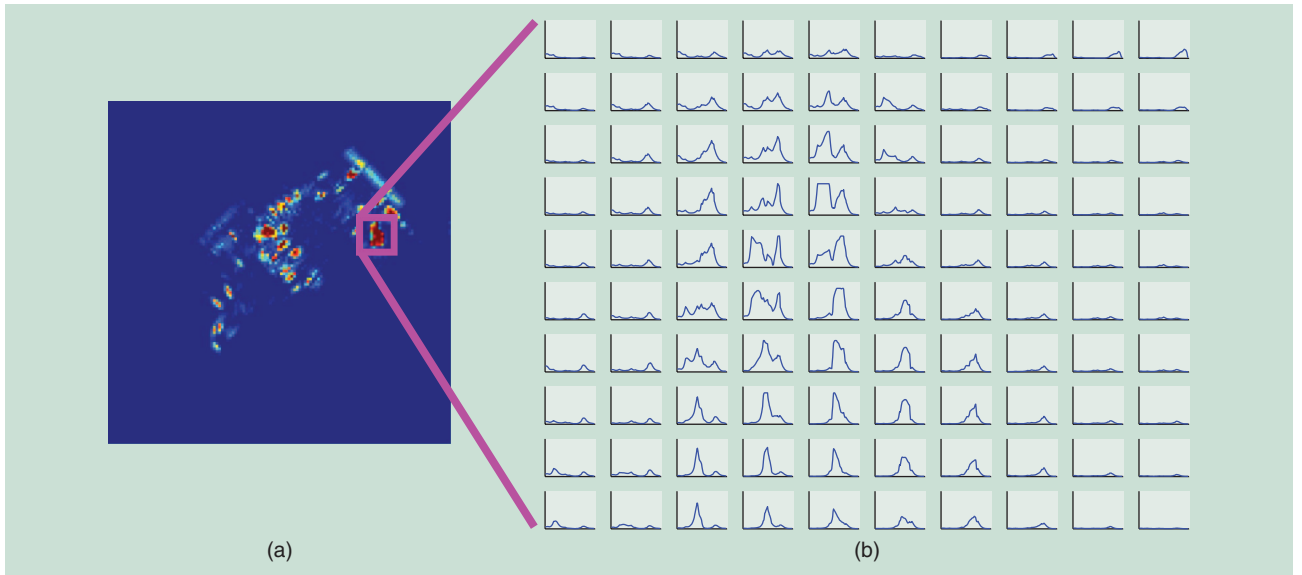
[FIG6] Anisotropy characterization for a subset of pixels in the backhoe loader using joint subaperture reconstruction imposing piecewise smoothness in angular scattering. The individual small plots in (b) have subaperture angle $\tilde{\theta}$ as the abscissa and the scattering magnitude $|s(\tilde{\theta})|$ as the ordinate. They are arranged to match the pixel locations in (a).

MOVING TARGET IMAGING

Joint SAR imaging and ground moving target localization has proven to be an important but challenging task due to an inherent ambiguity in target geolocation and velocity. While the components of the received signal belonging to a particular stationary target have the same phase in successive radar returns, the phase of a moving target varies due to its varying range. Hence, to the conventional SAR imager working under the assumption that the scene is stationary during aperture synthesis, motion amounts to phase errors and results in defocusing and even displacement of moving target energy. On the other hand, if the SAR imager assumes a particular nonzero scene motion, the moving target with a matching velocity appears focused, while all stationary and velocity mismatched targets appear defocused.
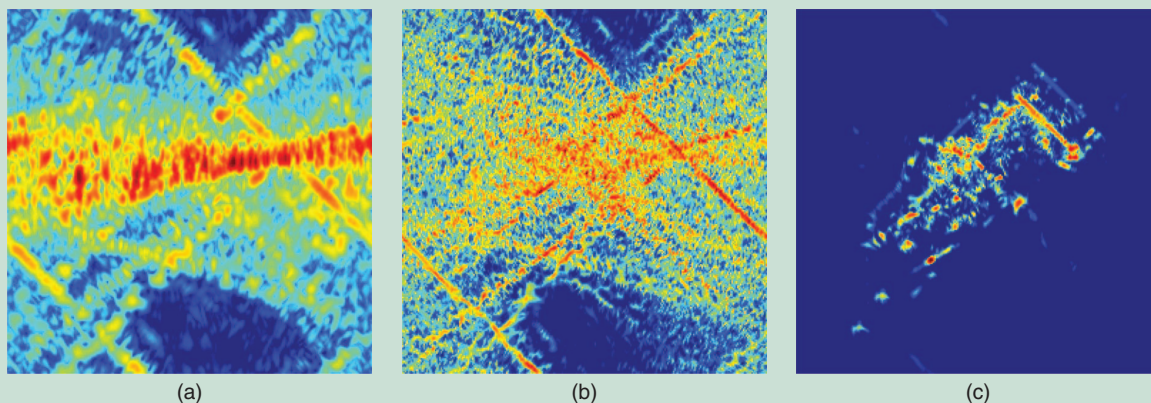
A common approach for SAR moving target imaging is first to find the smeared imagery of moving targets in a conventionally formed image and then perform phase error estimation and compensation for the corresponding image parts. Space-time adaptive processing uses data obtained from multiple channels to suppress clutter and separate moving targets from the background. Velocity SAR exploits phase information from multiple receive antennas, whereas dual-speed SAR processes the data collected by a platform flying with two different speeds in the radar observation duration.

Sparsity-based methods have recently made their way into moving target SAR imaging. In [38]–[41], sparse representation techniques are used to search for a solution over an overcomplete dictionary that consists of atoms for several velocity-position combinations. The overcomplete dictionary approach amounts to linearizing the nonlinear problem of target scattering and motion estimation and subsequently to solving the problem as a larger, unified regularized inversion problem involving sparsity constraints. A sample multistatic imaging result from [38] is illustrated in Figure 8. When a scene consisting of a stationary, a slowly moving, and a fast-moving target [shown in Figure 8(a) at time zero] is conventionally imaged under a zero-velocity assumption, the slowly moving target is defocused, while the fast-moving target disappears [Figure 8(b)]. The conventional reconstruction over a set of hypothesized velocities accurately localizes the moving targets, albeit with residual blur. Finally, Figure 8(d) shows that target features can be recovered by the sparsity-enforcing overcomplete dictionary approach [38]. In [40], a similar optimization problem to the one in [38] is solved after a clutter cancellation procedure is applied to the data.

Based on the observation that radar returns from a scene with motion can be viewed as data from a stationary scene, but with phase errors due to motion, a recently proposed idea is to view moving target imaging as a generalized, spatially variant autofocusing problem. The work in [42] does just that and extends the SDA framework, described in the previous section, to the problem of moving target imaging. Due to the spatially variant nature of the defocusing (due to the possibility of targets with different velocities at different locations), the number of unknowns is much greater than a basic autofocusing problem, making this a very ill-posed problem, requiring effective constraints for a successful solution. Based on this observation, [42] not only exploits the sparsity of the reflectivity field, but also imposes a constraint on the spatial sparsity of the phase errors based on the assumption that motion in the scene will be limited to a small number of spatial locations. The phase errors corresponding to all points in the scene, for all aperture positions are incorporated into the problem using the vector β, whose elements are in the form of $e^{j\epsilon}$'s. The following cost functional is minimized jointly with respect to the field and the phase errors:

$$J(\mathbf{s}, \beta) = \|\mathbf{r} - \mathbf{H}(\beta)\mathbf{s}\|_2^2 + \lambda_1\|\mathbf{s}\|_1$$
$$+ \lambda_2\|\beta - \mathbf{1}\|_1 \quad s.t. \; |\beta(i)| = 1 \;\; \forall i. \quad (13)$$

[FIG7] Imaging in the presence of phase errors uniformly distributed in $[-\pi, \pi]$. (a) Conventional imaging. (b) Sparsity-driven imaging without phase error compensation. (c) SDA.

Here, $\mathbf{1}$ is a vector of ones. Assuming that the number of moving points constitutes a small percentage of the total number of points in the scene, most of the ϵ values are zero, and subsequently most of the elements in the vector β are one. Therefore, this sparsity on the phase errors is incorporated into the problem formulation by using the regularization term $\|\beta - \mathbf{1}\|_1$. Results of an experiment on a synthetic scene containing two moving targets are shown in Figure 9. The six pointlike targets are stationary. To simulate the SAR returns from the two large targets moving with constant cross-range velocities, quadratic phase errors with a center to edge amplitude of π radians and 2.5π radians have been added to the data of these particular targets. These phase errors correspond to velocities of 2 m/s and 5 m/s, respectively, for the SAR system used in this experiment. Figure 9(a) and (b) show the results of conventional imaging and sparsity-driven imaging without phase error compensation, respectively. The result of sparsity-driven moving target imaging [42], displayed in Figure 9(c), shows the effectiveness of the method in removing the phase errors due to motion, as well as in producing an image that exhibits the qualities of sparsity-driven SAR imaging.

There exist several other pieces of recent work exploiting sparsity for moving target SAR imaging. The work in [39] concentrates on targets with micromotions that are mainly embodied with rotation and vibration. To enforce sparsity, generalized Gaussian and student-t prior models are considered, and the variational Bayes' approximation estimator is applied to the hierarchical Bayesian models involved in the problem. The paper [41] considers the problem of motion parameter estimation of moving targets with Doppler spectrum ambiguity and Doppler centroid frequency ambiguity encountered in SAR systems with low pulse repetition frequency, and presents a sparsity-based method that involves the use of the Radon transform to acquire unambiguous across-track velocities and range positions in the range profile domain. The paper [43] proposes an adaptive CS-based SAR system for dynamic sparse target scenes. The proposed system uses the recovered target scene information to detect if the scene has changed and optimizes the transmission waveform and sensing matrix accordingly. Finally, the paper [44] presents an approach that combines sparsity-driven radar imaging and change detection for detecting and localizing moving humans behind walls and inside enclosed structures.
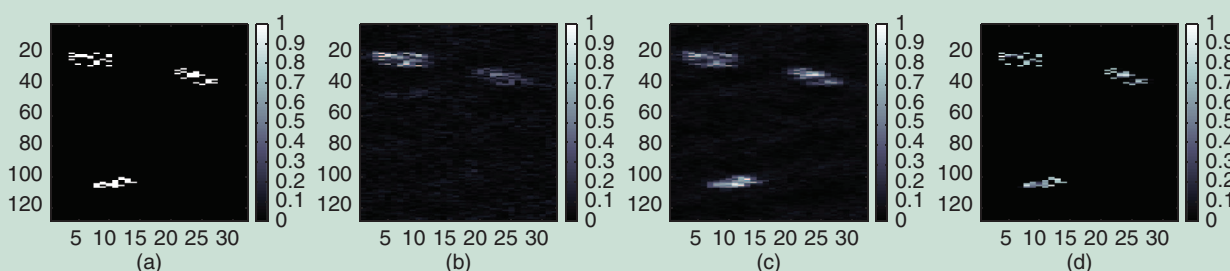
[FIG8] Multistatic moving target imaging. (a) A simulated ground truth scene at time $t = 0$. The upper left target is stationary, the upper right target moves slowly, and the bottom target moves at a faster velocity. (b) Conventional reconstruction when motion is ignored. (c) Conventional reconstruction over a set of velocity hypotheses. (d) Sparsity-enforcing overcomplete dictionary reconstruction. (Images used courtesy of [38].)
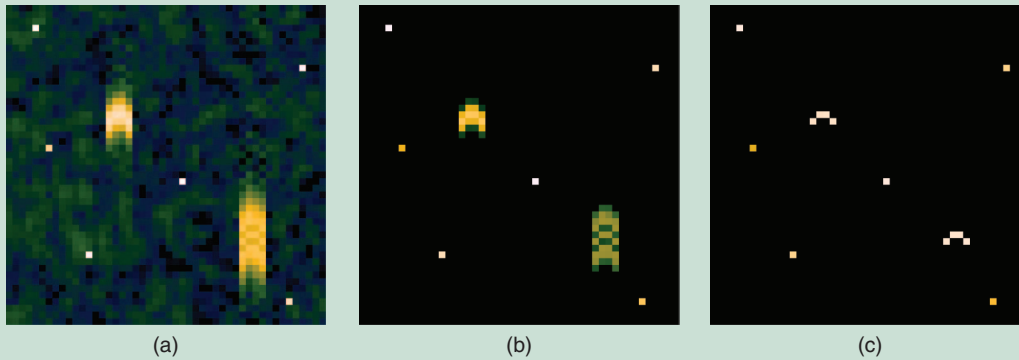
[FIG9] Imaging of a synthetic scene with moving targets. (a) Conventional imaging. (b) Sparsity-driven imaging assuming a stationary scene. (c) Joint sparsity-driven imaging and phase error correction.

COMPRESSED SENSING-BASED ANALYSIS AND DESIGN OF SAR SENSING MISSIONS

As discussed in previous sections, ideas based on sparse signal representation have led to advanced image formation methods that offer a number of benefits for SAR such as increased resolvability of point scatterers and reduced speckle, as well as robustness to limitations in data quality and quantity. Robustness to missing or undersampled data has recently become a particularly critical concern due to new mission requirements and sensor geometries that result in nondense and irregular sampling patterns in the SAR measurement space. Current radar systems are capable of accommodating multiple operational modes such as searching, tracking, and imaging on the same platform. Timeline constraints of a higher priority mode may require interrupts in SAR data collection and lead to gaps in the synthetic aperture. Likewise, jamming and interference from nearby transmitters may lead to frequency gaps in SAR data collection. Furthermore, multiplatform and passive sensing from transmitters of opportunity result in sparse sensing geometries and irregular sampling of the SAR measurement space. Such irregular and undersampled data scenarios motivate the application of CS [45] ideas and signal processing algorithms to SAR. Sparsity-driven methods described in previous sections serve as the main computational tool for inverting such limited data. In this section, we provide an overview of a subset of recent work on the use of CS theory and principles for analysis and design of monostatic and multistatic SAR sensing missions under various constraints on data collection.

CS seeks to acquire as few measurements as possible about an unknown signal, and given these measurements, reconstruct the signal either exactly or with provably small probability of error. Reconstruction methods used in CS involve sparsity-constrained, nonquadratic regularization ideas and algorithms similar to the ones discussed in previous sections. Based on CS theory, such methods can successfully recover the signal sampled well below the Nyquist rate provided that the signal has a sparse representation in some suitable domain and that its measurement process satisfies certain properties (such as incoherence [46]) with respect to the signal's sparsifying basis [45]. For example, signals sparse in the canonical basis (which is what we will assume in this section) can be

accurately reconstructed from measurements involving extremely few, but randomly chosen Fourier samples of a signal. Since both monostatic and multistatic SAR sensing can be viewed as obtaining samples of the spatial Fourier transform of the scattering field, these results open opportunities for reduced-data SAR sensing.

Random sampling of SAR data in 2-D Fourier space closely matches observation scenarios assumed in existing CS theory. While random subsampling can be primarily used to reduce onboard data storage requirements, it may not represent data limitations due to more structured interrupts and it may not enable reallocation of SAR sensing resources to other tasks. To enable such resource management and retasking, one could consider collecting returns of, e.g., a reduced number of transmitted waveforms by imposing randomness into the synthetic aperture [47], [48]. It would then be of interest to analyze and design sensing missions, i.e., practical data sampling configurations, based on the expected signal reconstruction quality and assess how well metrics appearing in CS theory (and that are defined by the measurement scenario) predict reconstruction performance from such limited data. Recent work on this question suggests CS principles may be used to analyze and guide the design of monostatic and multistatic SAR sensing missions under various constraints on data collection.

Here we provide highlights of such an analysis. One idea is to study sensitivity to data limitations and to the sampling patterns through mutual-coherence based metrics, which appear in CS theory. The mutual coherence of a measurement operator was proposed as a simple, but conservative measure of the ability of sparsity-enforcing reconstruction to accurately reconstruct a signal [46]. The mutual coherence of a complex-valued matrix $\mathbf{H}$, which in our case becomes the mutual coherence of a sensing configuration, is defined as

$$\mu(\mathbf{H}) = \max_{i \neq j} g_{ij}, \qquad g_{ij} = \frac{|\langle \mathbf{h}_i, \mathbf{h}_j \rangle|}{\|\mathbf{h}_i\|_2 \|\mathbf{h}_j\|_2}, i \neq j, \qquad (14)$$

where $\mathbf{h}_i$ is the ith column of the matrix $\mathbf{H}$, and the inner product is defined as $\langle \mathbf{h}_i, \mathbf{h}_j \rangle = \mathbf{h}_i^H \mathbf{h}_j$. The ith column vector $\mathbf{h}_i$ can be viewed as a range-aspect "steering vector" of a sensing

geometry or the contribution of a scatterer at a specific spatial location to the received phase history data. The mutual coherence measures the worst case correlation between responses of two distinct scatterers at different spatial locations. The $t_\%$-average mutual coherence, $\mu_{t\%}$, has been proposed as a measure more closely related to the average reconstruction performance of sparsity-driven SAR reconstruction [47]

$$\mu_{t\%}(\mathbf{H}) = \frac{\sum_{i\neq j} g_{ij}\mathcal{I}_{ij}(t_\%)}{\sum_{i\neq j}\mathcal{I}_{ij}(t_\%)}, \mathcal{I}_{ij}(t_\%) = \begin{cases} 1, & g_{ij} \in \varepsilon_{t_\%} \\ 0, & \text{otherwise,} \end{cases} \quad (15)$$

where $\varepsilon_{t_\%}$ denotes the set containing the largest $t\%$ column cross-correlations g_{ij}. Based on this definition, $\mu_{t\%}(\mathbf{H})$ measures the average cross-correlation value within the set of the $t_\%$ most similar column pairs. A large value of $\mu_{t\%}(\mathbf{H})$ indicates that there are many similar pairs of columns of $\mathbf{H}$ that can potentially confuse the reconstruction algorithm. This measure is more robust to outliers, which can unfairly dominate the mutual coherence. The $t\%$-mutual coherence can be related to the cumulative coherence [49] that, in the CS literature, has been used to derive sparse signal recovery conditions with convex cost function relaxations. The cumulative coherence provides an upper bound on the $t\%$-mutual coherence. Note that $\mu_{t\%}(\mathbf{H})$ can be computed for a sensing configuration before actual data collection. The question then is whether it can serve as a predictor of reconstruction quality of a sparse scene based on data to be collected through a particular configuration.

Figure 10 provides an example of the utility of $t_\%$-average mutual coherence on an urban scene from the publicly released Gotcha SAR data set [59]. Figure 10(a) shows the scatter plot of root-mean-square error (RMSE) of the reconstructions versus $\mu_{0.5\%}$ when the number of randomly missing aperture positions increases linearly up to 50%. Just for visualization, Figure 10(b) and (c) shows sample conventional and sparsity-driven reconstructions of the scene with 24% of the synthetic aperture missing. The result in Figure 10(a) indicates that configurations with sufficiently small values of the $t\%$-average mutual coherence achieve high-quality reconstruction and that $\mu_{0.5\%}$ appears to be a good predictor of reconstruction quality. This is an easily computed parameter that can be utilized for real-time evaluation of sensing configurations and task planning of multimode radars. Although we have considered a simple monostatic scenario here for simplicity, the analysis in [47] suggests that such a CS-motivated metric can be useful in the analysis and design of multistatic sensing missions as well. In the multistatic case, CS and sparsity-driven reconstruction have the potential to allow for sensing with fewer transmitted probes and reduced acquisition time.

Another way CS theory has recently impacted SAR imaging is by motivating the design of new radar waveforms. New radar waveforms such as Alltop and pseudorandom sequences have been shown to lead to high-resolution imaging radar and reduced analog-to-digital conversion bandwidth [7], [50]. Compressive sensing through convolution using random noiselike transmitted waveforms followed by random time-domain subsampling and its application to SAR was discussed in [51]. These waveforms result in incoherent radar sensing matrices and allow for accurate reconstruction of sparse target scenes. Multistatic and distributed radar waveform design for CS was discussed in [52]. CS for MIMO radars was addressed in scenarios involving uniform linear antenna array configurations [53], [54] and antennas randomly distributed over a small area [55].

SUMMARY AND DISCUSSION

We have presented an overview of recent lines of inquiry that lie at the intersection of two domains: sparse signal representation and SAR image formation. For basic SAR imaging, we have described image formation methods founded upon analysis and synthesis-based sparse signal representation ideas, and discussed how the complex-valued and potentially random-phase nature of SAR reflectivities have led to interesting optimization formulations different from those encountered in basic sparse signal representation problems. Motivated by emerging applications, including those involving sensing by unmanned aerial vehicles, we have considered the problem of wide-angle SAR imaging and described how exploitation of the sparsity of the scene and that of the angular scattering response can lead to effective imaging and anisotropy characterization. Then we have turned to the issue of phase errors, and described how exploitation of sparsity enables autofocusing in challenging conditions. We have pointed to
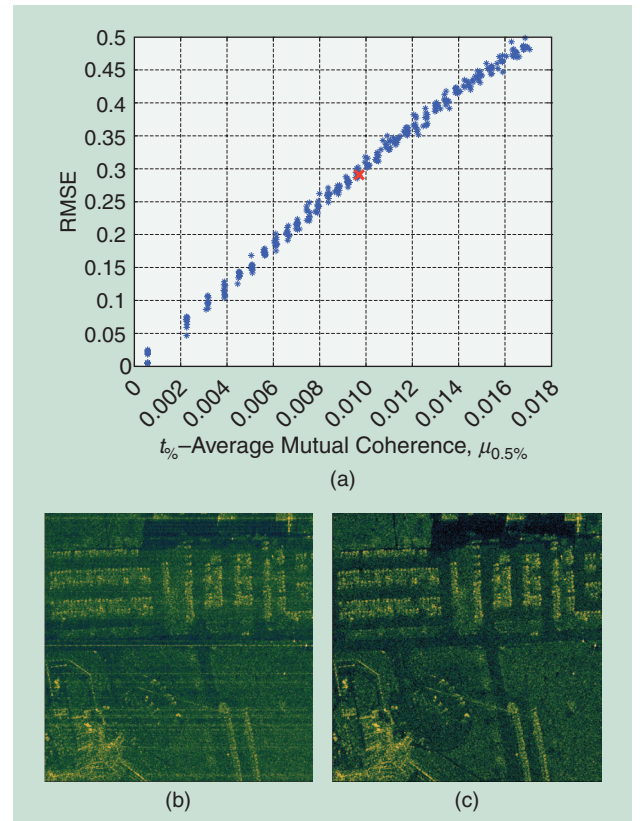
[FIG10] A compressed sensing-based analysis of sensing configurations. (a) RMSE versus $\mu_{0.5\%}$. (b) Conventional reconstruction, and (c) sparsity-driven reconstruction corresponding to the red point in (a) with 24% of missing data. (Images used courtesy of [47].)

recent pieces of work that attempt to use sparsity for the challenging problem of moving target SAR imaging. Finally, we have discussed how recent developments in CS theory have motivated not only the use of sparsity-driven methods for SAR imaging, but also the analysis and design of SAR sensing missions under physical, geometric, or temporal constraints on data collection.

The body of work on sparsity-driven SAR imaging we have covered here (and related pieces of work we were not able to cover due to space constraints), shows that sparsity can be a useful asset for SAR imaging especially in nonconventional data collection scenarios (e.g., when the data are sparse, irregular, limited) leading to severely underconstrained, ill-posed problems for image formation. Sparsity-driven imaging should not necessarily be viewed as a general-purpose approach that should replace more traditional SAR image formation methods completely. When used properly, it is a tool that can enable the radar engineer to extract interesting pieces of information from SAR data that is not possible through more conventional means. As any approach for solving an ill-posed problem, it relies on a certain type of assumption, which, in this particular case, is that the scene admits sparse representation in some domain. It performs very well on scenes that exhibit sparsity or compressibility, and enhances aspects of a particular scene that exhibit these characteristics. If the important characteristics of the scene and the sparse structure imposed through a particular dictionary are mismatched, we would obviously not expect the approach to produce improved imagery. This is why we expect "learning" to be an important theme in future work, as we describe below. Furthermore, when sparsity by itself is not sufficient to capture the rich information content of a scene, it might be possible to combine it with other types of priors each of which describes a component of a decomposed scene.

The research we have reviewed provides a principled basis and demonstrates how sparsity can be exploited in several contexts in SAR imaging. We believe we will witness wider utilization of sparsity-based methods in real SAR imaging applications over the upcoming years if several challenges are addressed and further research is carried out with a broader perspective. These challenges include reducing computational complexity, establishing stronger connections between imaging and decision-making, using effective machine-learning ideas to tune the notion of sparsity to a particular context, and going beyond sparsity to capture other forms of simple structures present in the data. Based on this perspective, we briefly describe four lines of research that we believe will enrich this problem domain and widen its applicability.

1) *Computational advances.* The first issue is computational complexity. While we might never expect sparsity-driven imaging to be as fast as simple Fourier transform-based imaging methods, more work is needed to develop exact and approximate algorithms that exploit the problem structure to produce faster solutions. One can think of several related research thrusts under this theme. First, given recent developments in convex optimization methods, it is of interest to adapt promising methods to particular SAR imaging problems to improve computational efficiency. As an example, augmented Lagrangian methods such as alternating direction method of multipliers could be considered not only because of their fast convergence properties, but also due to their potential for distributed implementation leading to parallelization. This brings us to our next point, which is whether one could exploit parallel processing on graphics processing units (GPUs) for sparsity-driven SAR imaging. While there exist GPU implementations of sparse signal representation ideas used as postprocessing despeckling methods, effective GPU implementations of the solution of the inverse problem for imaging is more challenging. Finally, for sparsity-driven SAR imaging problems involving large dictionaries, it is of interest to develop approximate algorithms that intelligently search the solution space exploiting the problem structure to achieve fast and reasonably accurate solutions. Advances in computational tools would enable wider utilization of sparsity-driven SAR imaging methods especially in relatively large problems involving, e.g, 3-D imaging in the context of TomoSAR.

2) *Decision-directed imaging.* We envision two potential major lines of inquiry suggesting the establishment of closer connections between SAR imaging and machine learning. The one we describe here involves the interplay between SAR imaging and further decision making. As discussed in the body of this article, one of the early motivations for sparsity-driven SAR imaging has been the preservation and enhancement of features important for tasks such as automatic target recognition. While this line of thinking has produced images with, e.g., better preservation of scatterer locations or easier to segment regions, accomplishments have been limited in at least to ways: first, only very low-level features have been used, and second, this has been an "open-loop" process. It would be interesting to bring in higher-level information, such as object shapes, into the problem formulation. It would also be interesting to take a decision-directed perspective and use information fed back from the inference engine, such as partial information on classes of objects in the scene, while solving the image formation problem. Whether one could formulate a sparse representation perspective to incorporate such high-level statistical information is a question worthy of exploration.

3) *Closer connections to machine learning.* Another major line of inquiry we foresee involves close integration of machine-learning methods into sparsity-driven SAR imaging. We have already mentioned that sparsity-driven imaging can be formulated using a Bayesian perspective that involves priors on the reflectivity field and the parameters, and in which the imaging problem involves characterizing a posterior density. While there exists some work with this perspective, using machine learning methods to demonstrate the benefits offered by such a statistical perspective is of interest for the future. Another aspect in which we expect learning methods to play a more prominent role is the construction of the dictionaries used in sparse representation. While there has been some preliminary work on dictionary learning in the context of SAR imaging, significant benefits are yet to be demonstrated. Connecting this back to decision-directed processing, one might consider performing discriminative dictionary learning as well.

4) *Other forms of "simplicity."* The final area of research we anticipate is about exploiting other types of structures potentially exhibited by SAR data in addition to sparsity. In particular, a concrete potential line of work could involve the use of low-rank models. Recent theoretical work on low-rank models shares many aspects of earlier work on sparsity and CS: low-rank matrix recovery problems are posed as optimization problems, relaxed forms of which, involving nuclear norms of matrices, are solved efficiently. Temporal and spatial dependencies in SAR data may lead to successful use of low-rank models, in a variety of contexts including moving target imaging and wide-angle imaging, and could possibly involve decomposition of some of the signals into sparse and low-rank components as well.

Overall, sparsity-driven SAR imaging is an exciting topic of study for both radar imaging experts and statistical signal processing researchers. Due to its connections to interesting ongoing theoretical work on signal representation and CS, as well as due to its potential for real impact on existing and emerging applications, we expect that it will continue to be an active area of academic and engineering development in the near future.

AUTHORS

Müjdat Çetin (mcetin@sabanciuniv.edu) is an associate professor at Sabancı University, İstanbul, Turkey. He was the technical program cochair for the International Conference on Information Fusion in 2013 and for the International Conference on Pattern Recognition in 2010. He has received several awards including the 2013 IET Radar, Sonar, and Navigation Premium Award, the 2010 IEEE Signal Processing Society Best Paper Award, the 2007 Elsevier Signal Processing Journal Best Paper Award, and the 2008 Turkish Academy of Sciences Distinguished Young Scientist Award. He was an associate editor of *IEEE Signal Processing Letters* and *IEEE Transactions on Cybernetics* from 2012 to 2014. He is currently an associate editor of *IEEE Transactions on Image Processing*. His current research interests include image reconstruction and restoration, brain–computer interfaces, biomedical information processing, and image analysis.

Ivana Stojanović (ivana.z.stojanovic@gmail.com) received the Dipl.Ing. degree from the University of Belgrade, Serbia, in 1999 and the M.S. and Ph.D. degrees in electrical engineering from Boston University in 2007 and 2012, respectively. At Boston University, she worked on sparse signal reconstruction and compressed sensing application to synthetic aperture radar imaging and biomedical signal processing. She is currently a lead research engineer at HERE, a Nokia business developing 3-D maps. Previously, she held a senior research scientist position at Scientific Systems Company, where she worked on interrupted synthetic aperture radar. From 1999 to 2005, she held positions in Iospan Wireless and Intel working as a wireless systems engineer developing WiMax systems.

N. Özben Önhon (onhon@sabanciuniv.edu) received the B.S. degree in electronics and telecommunication engineering and the M.S. degree in telecommunication engineering from İstanbul Technical University, in 2003 and 2006, respectively. She received the Ph.D. degree in electronics engineering from Sabancı University in 2012. She is currently a faculty member at Turkish–German University, İstanbul, Turkey. Her research interests are in the areas of signal and image processing.

Kush R. Varshney (krvarshn@us.ibm.com) received the B.S. degree in electrical and computer engineering with honors from Cornell University in 2004 and the S.M. and Ph.D. degrees, both in electrical engineering and computer science, from the Massachusetts Institute of Technology in 2006 and 2010, respectively. He is a research staff member in the Mathematical Sciences and Analytics Department at the IBM Thomas J. Watson Research Center. He received a Best Student Paper Travel Award at the 2009 International Conference on Information Fusion; the Best Paper Award at the 2013 IEEE International Conference on Service Operations and Logistics, and Informatics; and several IBM awards for contributions to business analytics projects. He is on the editorial board of *Digital Signal Processing* and a member of the IEEE Signal Processing Society Machine Learning for Signal Processing Technical Committee.

Sadegh Samadi (samadi@ sutech.ac.ir) is a faculty member at the Department of Electrical and Electronics Engineering, Shiraz University of Technology, Iran. He received the Ph.D. degree from Shiraz University, Iran, in 2010. He received the 2013 IET Radar, Sonar, and Navigation Premium Award. His research interests lie within the broad field of statistical signal and image processing.

W. Clem Karl (wckarl@bu.edu) received the Ph.D. degree in electrical engineering and computer science from the Massachusetts Institute of Technology. He is a professor of electrical and computer engineering and biomedical engineering at Boston University. He is currently the editor-in-chief of *IEEE Transactions on Image Processing* and a member of the IEEE Signal Processing Society's Conference Board. He is a past member of the Society's Board of Governors and was the general chair of the 2009 IEEE International Symposium on Biomedical Imaging. His current research interests include statistical image processing, estimation, detection, and inverse problems, such as tomography.

Alan S. Willsky (willsky@mit.edu) is the E.S. Webster professor of electrical engineering and computer science at the Massachusetts Institute of Technology and was a founder of Alphatech, Inc. Among his awards are the 1975 American Automatic Control Council Eckman Award, 1979 American Society of Civil Engineers Alfred Noble Prize, 1980 IEEE Browder Thompson Award, 2004 IEEE Donald Fink Prize Paper Award, Doctorat Honoris Causa from Université de Rennes, 2009 Technical Achievement and 2014 Society Awards from the IEEE Signal Processing Society. He is a member of the National Academy of Engineering and is a coauthor of *Signals and Systems*. His research interests are in the development and application of methods of estimation, machine learning, and statistical signal and image processing.

REFERENCES

[1] J. Ender, "On compressive sensing applied to radar," *Signal Process.*, vol. 90, no. 5, pp. 1402–1414, May 2010.

[2] L. C. Potter, E. Ertin, J. T. Parker, and M. Çetin, "Sparsity and compressed sensing in radar imaging," *Proc. IEEE*, vol. 98, no. 6, pp. 1006–1020, June 2010.

[3] M. Çetin and W. C. Karl, "Feature-enhanced synthetic aperture radar image formation based on nonquadratic regularization," *IEEE Trans. Image Processing*, vol. 10, no. 4, pp. 623–631, Apr. 2001.

[4] M. Çetin, W. C. Karl, and D. A. Castañón, "Feature enhancement and ATR performance using non-quadratic optimization-based SAR imaging," *IEEE Trans. Aerosp. Electron. Syst.*, vol. 39, no. 4, pp. 1375–1395, Oct. 2003.

[5] S. I. Kelly, C. Du, G. Rilling, and M. E. Davies, "Advanced image formation and processing of partial synthetic aperture radar data," *IET Signal Process.*, vol. 6, no. 5, pp. 511–520, July 2012.

[6] Z. Wang and W. Wang, "Fast and adaptive method for SAR superresolution imaging based on point scattering model and optimal basis selection," *IEEE Trans. Image Processing*, vol. 18, no. 7, pp. 1477–1486, July 2009.

[7] R. Baraniuk and P. Steeghs, "Compressive radar imaging," in *Proc. IEEE Radar Conf.*, Waltham, MA, Apr. 2007, pp. 128–133.

[8] M. Ferrara, J. A. Jackson, and C. Austin, "Enhancement of multi-pass 3D circular SAR images using sparse reconstruction techniques," in *Algorithms for Synthetic Aperture Radar Imagery XVI*, ser. Proc. SPIE, E. G. Zelnio and F. D. Garber, Eds., vol. 7337, Orlando, FL, Apr. 2009, p. 733702.

[9] S. Samadi, M. Çetin, and M. A. Masnadi-Shirazi, "Sparse representation-based synthetic aperture radar imaging," *IET Radar, Sonar Navigat.*, vol. 5, no. 2, pp. 182–193, Feb. 2011.

[10] I. Stojanović, "Sparse reconstruction in monostatic and multistatic SAR," Ph.D. dissertation, Dept. Electrical and Comput. Engin., Boston Univ., 2012.

[11] L. C. Potter, P. Schniter, and J. Ziniel, "Sparse reconstruction for radar," in *Algorithms for Synthetic Aperture Radar Imagery XV*, ser. Proc. SPIE, E. G. Zelnio and F. D. Garber, Eds., vol. 6970, Orlando, FL, Mar. 2008, p. 697003.

[12] G. Xu, M. Xing, L. Zhang, Y. Liu, and Y. Li, "Bayesian inverse synthetic aperture radar imaging," *IEEE Geosci. Remote Sensing Lett.*, vol. 8, no. 6, pp. 1150–1154, Nov. 2011.

[13] O. Batu and M. Cetin, "Parameter selection in sparsity-driven SAR imaging," *IEEE Trans. Aerosp. Electron. Syst.*, vol. 47, no. 4, pp. 3040–3050, Oct. 2011.

[14] M. Çetin and A. Lanterman, "Region-enhanced passive radar imaging," *IEE Proc. Radar, Sonar Navigat.*, vol. 152, no. 3, pp. 185–194, June 2005.

[15] X. Tan, W. Roberts, J. Li, and P. Stoica, "Sparse learning via iterative minimization with application to MIMO radar imaging," *IEEE Trans. Signal Processing*, vol. 59, no. 3, pp. 1088–1101, Mar. 2011.

[16] W. Rao, G. Li, X. Wang, and X.-G. Xia, "Adaptive sparse recovery by parametric weighted L_1 minimization for ISAR imaging of uniformly rotating targets," *IEEE J. Select. Topics Appl. Earth Observ. Remote Sensing*, vol. 6, no. 2, pp. 942–952, Apr. 2013.

[17] M. G. Amin and F. Ahmad, "Compressive sensing for through-the-wall radar imaging," *J. Electron. Imag.*, vol. 22, no. 3, p. 030901, July 2013.

[18] N. Ramakrishnan, E. Ertin, and R. Moses, "Enhancement of coupled multichannel images using sparsity constraints," *IEEE Trans. Image Processing*, vol. 19, no. 8, pp. 2115–2126, Aug. 2010.

[19] A. Budillon, A. Evangelista, and G. Schirinzi, "Three-dimensional SAR focusing from multipass signals using compressive sampling," *IEEE Trans. Geosci. Remote Sensing*, vol. 49, no. 1, pp. 488–499, Jan. 2011.

[20] X. X. Zhu and R. Bamler, "Tomographic SAR inversion by L_1-norm regularization—The compressive sensing approach," *IEEE Trans. Geosci. Remote Sensing*, vol. 48, no. 10, pp. 3839–3846, Oct. 2010.

[21] J. Jackson and R. Moses, "Synthetic aperture radar 3D feature extraction for arbitrary flight paths," *IEEE Trans. Aerosp. Electron. Syst.*, vol. 48, no. 3, pp. 2065–2084, July 2012.

[22] W. G. Carrara, R. M. Majewski, and R. S. Goodman, *Spotlight Synthetic Aperture Radar: Signal Processing Algorithms*. Norwood, MA: Artech House, 1995.

[23] R. L. Moses, L. Potter, and M. Çetin, "Wide angle SAR imaging," in *Algorithms for Synthetic Aperture Radar Imagery XI*, ser. Proc. SPIE, E. G. Zelnio and F. D. Garber, Eds., vol. 5427, Orlando, FL, Apr. 2004, pp. 164–175.

[24] A. Fasoula, H. Driessen, and P. van Genderen, "De-ghosting of tomographic images in a radar network with sparse angular sampling," in *Proc. European Radar Conf.*, Rome, Italy, Sept.–Oct. 2009, pp. 286–289.

[25] C. D. Austin, E. Ertin, and R. L. Moses, "Sparse signal methods for 3-D radar imaging," *IEEE J. Select. Topics Signal Processing.*, vol. 5, no. 3, pp. 408–423, June 2011.

[26] K. R. Varshney, M. Çetin, J. W. Fisher III, and A. S. Willsky, "Sparse representation in structured dictionaries with application to synthetic aperture radar," *IEEE Trans. Signal Processing*, vol. 56, no. 8, pp. 3548–3561, Aug. 2008.

[27] I. Stojanović, M. Çetin, and W. C. Karl, "Joint space aspect reconstruction of wide-angle SAR exploiting sparsity," in *Algorithms for Synthetic Aperture Radar Imagery XV*, ser. Proc. SPIE, E. G. Zelnio and F. D. Garber, Eds., vol. 6970, Orlando, FL, Mar. 2008, p. 697005.

[28] G. B. Hammond and J. A. Jackson, "SAR canonical feature extraction using molecule dictionaries," in *Proc. IEEE Radar Conf.*, Ottawa, Canada, Apr.–May 2013.

[29] T. C. Calloway and G. Donohoe, "Subaperture autofocus for synthetic aperture radar," *IEEE Trans. Aerosp. Electron. Syst.*, vol. 30, no. 2, pp. 617–621, Apr. 1994.

[30] C. V. Jakowatz, D. E. Wahl, P. S. Eichel, D. C. Ghiglia, and P. A. Thompson, *Spotlight-Mode Synthetic Aperture Radar: A Signal Processing Approach*. Norwell, MA: Kluwer Academic, 1996.

[31] J. H. G. Ender, "Autofocusing ISAR images via sparse representation," in *Proc. European Conf. Synthetic Aperture Radar*, Nuremberg, Germany, Apr. 2012, pp. 203–206.

[32] J. Duan, L. Zhang, and M. Xing, "A weighted eigenvector autofocus method for sparse-aperture ISAR imaging," *EURASIP J. Adv. Signal Process.*, vol. 2013, p. 92, Apr. 2013.

[33] T. Jihua and Z. Bingchen, "Motion compensation for compressive sensing SAR imaging with autofocus," in *Proc. IEEE Conf. Industrial Electronics and Applications (ICIEA)*, Beijing, China, June 2011, pp. 1564–1567.

[34] N. O. Önhon and M. Çetin, "A sparsity-driven approach for joint SAR imaging and phase error correction," *IEEE Trans. Image Processing*, vol. 21, no. 4, pp. 2075–2088, Apr. 2012.

[35] S. I. Kelly, M. Yaghoobi, and M. E. Davies, "Auto-focus for under-sampled synthetic aperture radar," in *Proc. Sensor Signal Processing for Defence (SSPD)*, London, Sept. 2012.

[36] S. Ugur and O. Arikan, "SAR image reconstruction and autofocus by compressed sensing," *Digital Signal Process.*, vol. 22, no. 6, pp. 923–932, Dec. 2012.

[37] S.-J. Wei and X.-L. Zhang, "Sparse autofocus recovery for under-sampled linear array SAR 3-D imaging," *Prog. Electromagn. Res.*, vol. 140, pp. 43–62, 2013.

[38] I. Stojanović and W. Karl, "Imaging of moving targets with multi-static SAR using an overcomplete dictionary," *IEEE J. Select. Topics Signal Processing*, vol. 4, no. 1, pp. 164–176, Feb. 2010.

[39] S. Zhu, A. M. Djafari, H. Wang, B. Deng, X. Li, and J. Mao, "Parameter estimation for SAR micromotion target based on sparse signal representation," *EURASIP J. Adv. Signal Process.*, vol. 2012, p. 13, Jan. 2012.

[40] A. S. Khwaja and J. Ma, "Applications of compressed sensing for SAR moving-target velocity estimation and image compression," *IEEE Trans. Instrum. Meas.*, vol. 60, no. 8, pp. 2848–2860, Aug. 2011.

[41] Q. Wu, M. Xing, C. Qiu, B. Liu, Z. Bao, and T.-S. Yeo, "Motion parameter estimation in the SAR system with low PRF sampling," *IEEE Geosci. Remote Sensing Lett.*, vol. 7, no. 3, pp. 450–454, 2010.

[42] N. Ö. Önhon and M. Çetin, "SAR moving target imaging in a sparsity-driven framework," in *Proc. SPIE Optics+Photonics, Wavelets and Sparsity XIV*, ser. Proc. SPIE, M. Papadakis, D. Van De Ville, and V. K. Goyal, Eds., 2011, vol. 8138, p. 813806.

[43] J. Zhang, D. Zhu, and G. Zhang, "Adaptive compressed sensing radar oriented toward cognitive detection in dynamic sparse target scene," *IEEE Trans. Signal Processing*, vol. 60, no. 4, pp. 1718–1729, Apr. 2012.

[44] F. Ahmad and M. Amin, "Through-the-wall human motion indication using sparsity-driven change detection," *IEEE Trans. Geosci. Remote Sensing*, vol. 51, no. 2, pp. 881–890, Feb. 2013.

[45] D. L. Donoho, "Compressed sensing," *IEEE Trans. Inform. Theory*, vol. 52, no. 4, pp. 1289–1306, Apr. 2006.

[46] D. L. Donoho and M. Elad, "Optimally sparse representation in general (nonorthogonal) dictionaries via ℓ_1 minimization," *Proc. Natl. Acad. Sci.*, vol. 100, no. 5, pp. 2197–2202, Mar. 2003.

[47] I. Stojanović, M. Çetin, and W. C. Karl, "Compressed sensing of monostatic and multistatic SAR," *IEEE Geosci. Remote Sensing Lett.*, vol. 10, no. 6, pp. 1444–1448, June 2013.

[48] V. Patel, G. Easley, D. Healy, and R. Chellappa, "Compressed synthetic aperture radar," *IEEE J. Select. Topics Signal Processing*, vol. 4, no. 2, pp. 244–254, Apr. 2010.

[49] J. Tropp, "Just relax: Convex programming methods for identifying sparse signals in noise," *IEEE Trans. Inform. Theory*, vol. 52, no. 3, pp. 1030–1051, Mar. 2006.

[50] M. Herman and T. Strohmer, "High-resolution radar via compressed sensing," *IEEE Trans. Signal Processing*, vol. 57, no. 6, pp. 2275–2284, June 2009.

[51] J. Romberg, "Compressive sensing by random convolution," *SIAM J. Imag. Sci.*, vol. 2, no. 4, pp. 1098–1128, Oct. 2009.

[52] N. Subotic, B. Thelen, K. Cooper, W. Buller, J. Parker, J. Browning, and H. Beyer, "Distributed RADAR waveform design based on compressive sensing considerations," in *Proc. IEEE Radar Conf.*, Rome, Italy, May 2008.

[53] C. Chen and P. Vaidyanathan, "Compressed sensing in MIMO radar," in *Proc. Asilomar Conf. Signals, Systems and Computers*, Pacific Grove, CA, Oct. 2008, pp. 41–44.

[54] T. Strohmer and B. Friedlander, "Compressed sensing for MIMO radar—Algorithms and performance," in *Proc. Asilomar Conf. Signals, Systems and Computers*, Pacific Grove, CA, Nov. 2009, pp. 464–468.

[55] Y. Yu, A. Petropulu, and H. Poor, "MIMO radar using compressive sampling," *IEEE J. Select. Topics Signal Processing*, vol. 4, no. 1, pp. 146–163, Feb. 2010.

[56] Air Force Research Laboratory, Sensor Data Management System, Moving and Stationary Target Acquisition and Recognition (MSTAR) data set. [Online]. Available: https://www.sdms.afrl.af.mil/index.php?collection=mstar

[57] Astrium TerraSAR-X sample imagery. [Online]. Available: http://www.astrium-geo.com/en/23-sample-imagery

[58] Air Force Research Laboratory, Sensor Data Management System, Civilian Vehicle Radar Data Domes. [Online]. Available: https://www.sdms.afrl.af.mil/index.php?collection=cv_dome

[59] Air Force Research Laboratory, Sensor Data Management System, Gotcha Volumetric SAR data set. [Online]. Available: https://www.sdms.afrl.af.mil/index.php?collection=gotcha

[SP]